# Noise simulation system for determining imaging conditions in digital radiography

R. Tanaka[*a], K. Ichikawa[a], K. Matsubara[a], H. Kawashima[b]
[a] School of Health Sciences, College of Medical, Pharmaceutical and Health Sciences, Kanazawa University, 5-11-80 Kodatsuno, Kanazawa, Japan 920-0942
[b] Department of Radiology, Kanazawa University Hospital, 13-1 Takara-machi, Kanazawa, Japan 920-8641

## ABSTRACT

Reduction of exposure dose and improvement in image quality can be expected to result from advances in the performance of imaging detectors. We propose a computerized method for determining optimized imaging conditions by use of simulated images. This study was performed to develop a prototype system for image noise and to ensure consistency between the resulting images and actual images. An RQA5 X-ray spectrum was used for determination of input-output characteristics of a flat-panel detector (FPD). The number of incident quantum to the detector per pixel (counts/pixel) was calculated according to the pixel size of the detector and the quantum number in RQA5 determined in IEC6220-1. The relationship among tube current-time product (mAs), exposure dose (C/kg) at the detector surface, the number of incident quanta (counts/pixel), and pixel values measured on the images was addressed, and a conversion function was then created. The images obtained by the FPD was converted into a map of incident quantum numbers and input into random-value generator to simulate image noise. In addition, graphic user interface was developed to observe images with changing image noise and exposure dose levels, which have trade-off relationship. Simulation images provided at different noise levels were compared with actual images obtained by the FPD system. The results indicated that image noise was simulated properly both in objective and subjective evaluation. The present system could allow us to determine necessary dose from image quality and also to estimate image quality from any exposure dose.

**Keywords:** Digital x-ray imaging, image quality, exposure dose, image simulation, flat panel detector (FPD)

## 1. INTRODUCTION

Digital X-ray imaging systems have been commonly used in place of analog systems in clinical practice. In a conventional analog system, imaging conditions needed to be adjusted to provide the necessary film density. In contrast, in a digital system, the image quality is assured to some extent by post image processing even if the imaging was not performed under appropriate conditions. That is, it is necessary to have the concern about imaging conditions more than in an analog imaging system to avoid an excessive patient dose. In addition, a reduction of the exposure dose and improvement in image quality can be expected to result from advances in the performance of imaging detectors. However, there have not been enough investigations for providing optimized imaging conditions in digital radiography.

In general, imaging conditions are customized empirically by trial and error on the basis of general parameters, radiation measurements, and image observations in each institution. There is another approach for determining imaging conditions based on experience and intuition, which is discouraged because of a lack of evidence for decision. In this study, we propose a computerized method for determining optimized imaging conditions by use of simulated images. The proposed method would allow us to determine the necessary dose from the image quality and also to estimate the image quality from the exposure dose, so that imaging conditions can be set appropriately without actual imaging. Our purpose in this study was to develop a prototype system for providing simulation images and to ensure consistency between the resulting images and actual images.

* rie44@mhs.mp.kanazawa-u.ac.jp; phone/fax 81 76 265-2537

## 2. MATERIALS AND METHODS

### 2.1 Imaging system

An indirect-type (CsI) flat-panel detector (FPD) system (PLAUDR C50, Konica Minolta, Japan) with an X-ray generator (UD150L-40E, Shimadzu, Japan) was used in this study. The matrix size was 3072×3072 pixels, the pixel size was 0.139×0.139 mm, the range of grayscale was 12 bits, and the field of view was 43.2×43.2 cm. The pixel scaling was linear with respect to exposure. The source-to-target distance (SID) was limited to 1.5 or 1.15 m in the system.

### 2.2 Measurement of input-output characteristics

An RQA5 X-ray spectrum was used for determination of input-output characteristics according to IEC62220-1 [1, 2]. In our system, it was realized with 21 mm Al additional filtration at 74 kV. All measurements were conducted without grid in front of the detector. Image preprocessing consisted of offset and gain correction as well as compensation for defective or nonlinear pixels, as applied in normal clinical use of the detector.

The air kerma values were measured free-in-air in the detector plane with an ionization chamber (AE-132a 2902209; Oyogiken Inc., Tokyo, Japan). The SID was set in 1.5 and the ionization chamber was placed 500 mm behind the detector. The exposure dose was measured from 0.5 mAs to 120 mAs, and images were obtained. The measurements were performed three times at each dose level, and the average air kerma was calculated. The air kerma at the detector surface was calculated by the inverse-square distance law.

Regions of interest (ROIs) were located manually near the detector center on images, 100×100 pixels in size, and average pixel values were measured with Image-J ver. 1.42 (http://rsb.info.nih.gov/ij/) in each ROI. Input-output characteristics were plotted so that the linearity between the exposure dose and pixel values was confirmed (Fig. 1).

### 2.3 Creation of conversion function

The relationship among the tube current-time product (mAs), exposure dose (C/kg) at the detector surface, the number of incident quanta (counts/pixel), and pixel values measured on the images was addressed, and a conversion function was then created by fitting of the results to a linear function, y=a+bx. The conversion function for imaging an object was created as well. The incident quantum numbers through the object (acrylic plate, thickness; 15 mm, density; 1.19 g/cm3, attenuation coefficient; 2.07×10-2 $m^2$/kg) was calculated as follows;

$$I = I_0 \cdot \mathrm{e}^{-\mu x}, \qquad (1)$$

Where $I_0$ and $I$ are incident quantum number at the detector surface and at a depth of $x$ m, and $\mu$ is linear attenuation coefficient[3,4].

### 2.4 Simulation of image noise

Image noise was induced by statistical fluctuation of the quanta incident to the detector, which followed a Poisson distribution. Thus, for simulation of image noise, the map of incident quantum numbers was input into the Poisson random-number generator in each pixel [5, 6].

The image obtained at which the pixel values became saturated was used as an input image to our simulation system. In this study, it was 63 mAs (100 mA, 630 msec, SID=150 cm) at the exposure quality of RQA5. The image was converted into a map of incident quantum numbers by use of the conversion function as shown in Fig. 2. The incident quantum numbers were changed by multiplying the map by a weighting factor for simulation of images at various noise levels. Each pixel in the weighted map was input into the random-value generator. The output values from the random number generator were again converted into pixel values through the conversion function. The final output image was noise simulation image.

### 2.5 Development of prototype system

Our prototype system was developed on a personal computer (CPU, Pentium 4, 2.6 GHz; Memory, 2 GB; operating system, Windows XP; Microsoft, Redmond, WA) (Development environment, C++Builder; Borland, Scotts Valley, CA).

We created look-up table (LUT) to associate the pixel value with the exposure dose by using the conversion function as shown in Fig. 2. The LUT was installed in the simulation system with a graphic user interface (GUI) which indicates the necessary exposure dose (mR) and tube current-time product (mAs) to provide the necessary image quality in diagnosis.

### 2.6 Validation of the developed system

For ensuring the consistency between simulation and actual images, simulation images were compared with actual images provided by use of the FPD system at different noise levels of 0.85×10-7 C/kg (0.33 mR), 2.84×10-7 C/kg (1.06 mR), and 8.02×10-7 C/kg (3.11 mR). In this preliminary study, the developed system was examined under fixed conditions of 74 kV (RQA5) and SID=150 cm.

#### 2.6.1 Objective evaluation

The NPS was measured in the simulation flat-field images and compared with those of the actual flat-field images at the three different dose levels mentioned above (74 kV, 100 mA, SID=150 cm). Average pixel values measured in region of interest (ROI, 256×256 pixels in size) near the detector center were converted to the quantum numbers by use of the conversion function as shown in Fig. 2. The quantum numbers were input into a random-number generator for creation of simulation images at each noise level. The NPS of the simulation and actual images were calculated according to IEC62220-1 [2], and the results were compared at each exposure levels.

#### 2.6.2 Subjective evaluation

Images of barger phantom (acrylic plate with concave ditches, thickness; 15 mm, ditch diameter; 0~10 mm, ditch depth; 0.5~10mm) were obtained at the three exposure dose levels. An image of the barger phantom was also obtained at the exposure level at which the pixel values become saturated, 18×10-7 C/kg (6.96 mR), to be used as an input image into the simulation system. Simulation images were provided from the input image through the conversion function and random number generator.

An observer study was conducted to ensure the visual consistency between the simulated and actual images by six radiological technologists. A pair of actual and simulation images were prepared at three exposure levels. They were displayed on a 2M monochrome liquid crystal display (LCD) (RadiForce GS220, EIZO, Japan) and compared in terms of the detection of signals in the barger phantom images. The window level and width of the images were adjusted to the average pixel value of the images and double the window level, respectively. The observation distance and time were set depending on each observer; however, the room brightness was maintained at 50 lx. The minimum diameter and depth of the ditch were determined which could be detected with a confidence of 50 %. Image quality figures (IQF) were calculated based on the resulting contrast- detail (C-D) curves as shown in Fig. 3 [7]. The IQF was calculated as follows;

$$IQF = \frac{n}{\sum_{i=1}^{n} C_i \cdot D_{i.\min}} \quad , \qquad (2)$$

where *Ci*, *Di*, and *n* are the depth and diameter of each ditch, and the number of steps, respectively. A larger IQF means better image quality.

# 3. RESULTS

### 3.1 Objective evaluation

The average NPS of actual image at each dose level were $4.90\times10^{-6}$, $6.77\times10^{-6}$, and $3.75\times10^{-5}$ and those of the simulation image were $1.10\times10^{-6}$, $4.53\times10^{-6}$, and $4.41\times10^{-5}$. There were some differences between NPS of the actual and the simulation image at the same exposure level, and the maximum difference was $0.66\times10^{-5}$.

### 3.2 Subjective evaluation

Figure 3 barger phantom images of the actual images and the simulation images at each exposure level. Figure 4 shows C-D curves obtained at our observer study. Table 1 shows the average IQF of 6 observers, calculated from C-D curves. In an observer study, both images showed almost the same signal detectability, which decreased with decreasing exposure dose. There was no significant difference between actual images and simulation images at the same exposure dose level ($P<0.01$), although there were differences between different exposure dose levels.

### 3.3 Estimation of exposure dose

Figure 5 shows the GUI of the system we developed. The GUI was very useful for observation of images changing image noise and exposure dose levels, which have a trade-off relationship.

# 4. DISCUSSION

It was confirmed that image noise was simulated almost properly in objective and subjective evaluation. The simulation system with GUI was useful to observe images with changing image noise and exposure dose levels. Although under restricted imaging conditions, the feasibility of simulation approach to optimize imaging conditions was indicated. However, there were some differences in NPS of actual images through spatial frequencies, in contrast, simulation images showed almost the same NPS through spatial frequencies. These results indicated that simulation images could not simulate the other noise factor, such as electrical noise and structural noise, which were involved in the actual images. Further studies are required to expand the present system to be involved influences of these noise factors, along with adding wide range of initial data in X-ray tube voltage (exposure quality), SID, and object thickness to improve the performance of the present system.

# 5. CONCLUSION

We developed an image noise simulation system with a GUI to observe images with changing image noise and exposure dose levels, which have a trade-off relationship. Simulation images were compared with the actual images physically, and visually and the consistency between them was confirmed. The results suggested that the appropriate exposure dose could be determined from necessary image quality using the present system. The simulation approach is expected to be very useful to optimize imaging conditions in digital X-ray imaging systems.

Acknowledgements

This work was supported in part by a research grant from the Japanese Society of Medical Physics (JSMP).

Table 1. The average IQF of 6 observers

| | **0.33mR** | **1.06mR** | **3.11mR** |
|---|---|---|---|
| Actual image | $0.11 \pm 0.01$ | $0.13 \pm 0.03$ | $0.16 \pm 0.03$ |
| Simulation image | $0.10 \pm 0.01$ | $0.13 \pm 0.03$ | $0.16 \pm 0.03$ |

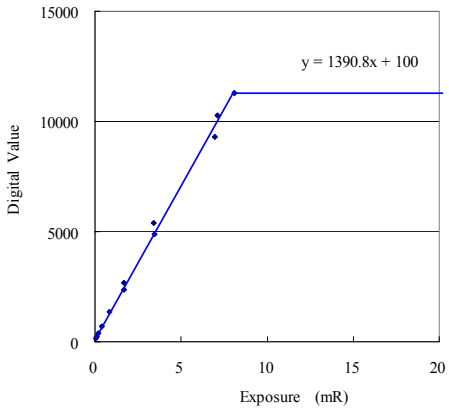


Figure 1 Input-output characteristics

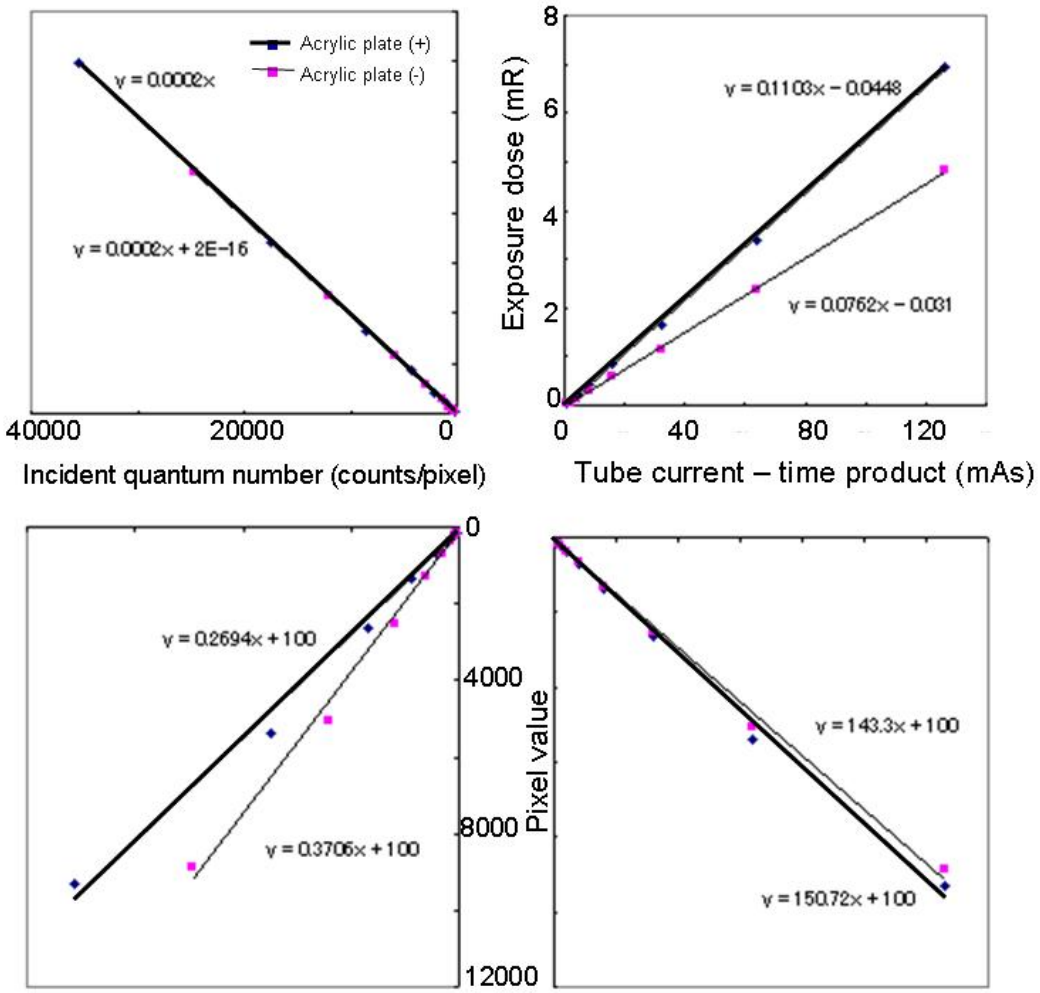


Figure 2 Relationship among tube current-time product (mAs), exposure dose (C/kg) at the detector surface, quantum number per pixel (counts/pixel), and pixel values measured on images (RQA5 X-ray spectrum of HVL=7.1 mm Al, realized with 21 mm Al additional filtration at 74 kV in SID150cm)

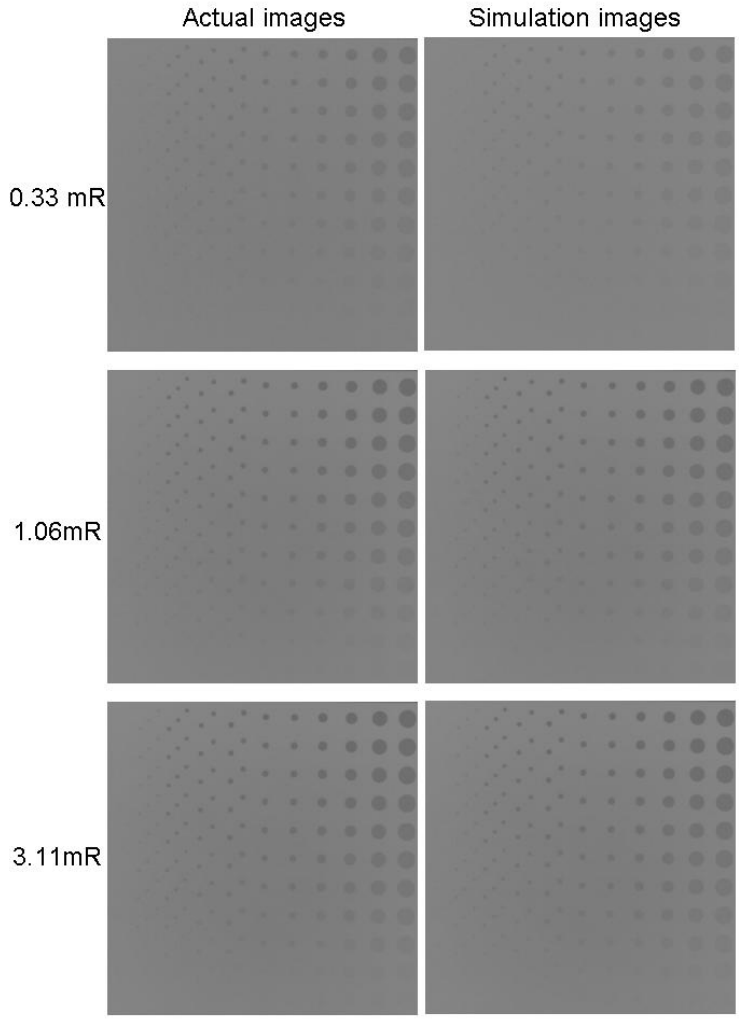


Figure 3 Barger phantom images provided by the FPD system (Upper) and simulation system (Lower) at the exposure dose of 0.85×10-7C/kg (0.33 mR), 2.84×10-7C/kg (1.06mR), and 8.02×10-7C/kg (3.11mR).

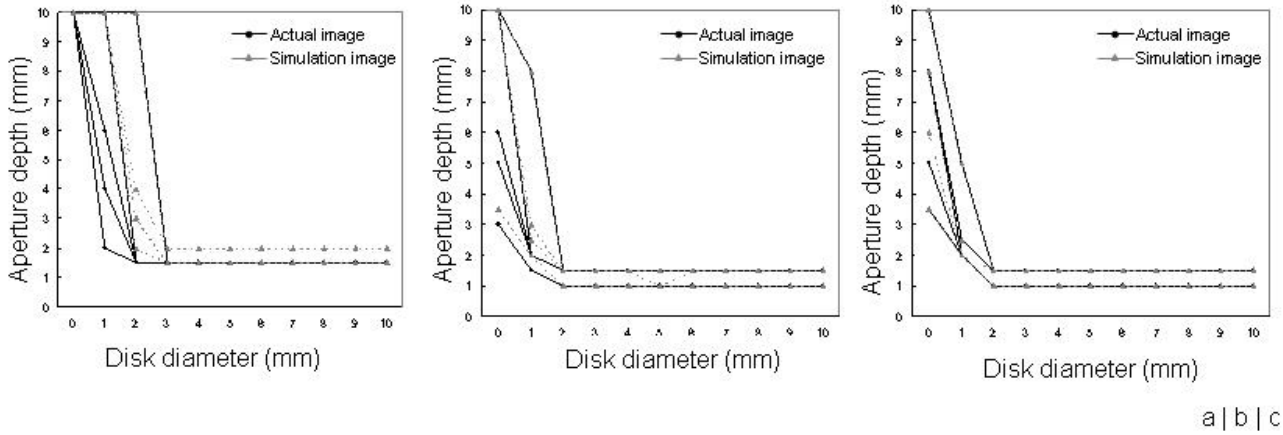


Figure 4 Contrast-detail curves of actual images provided using a FPD system and simulation images at the exposure dose of (a) 0.85 $\times 10^{-7}$C/kg (0.33 mR), (b) 2.84$\times 10^{-7}$C/kg (1.06mR), and (c) 8.02$\times 10^{-7}$C/kg (3.11mR) (n=6). Error bars show +/-SD.

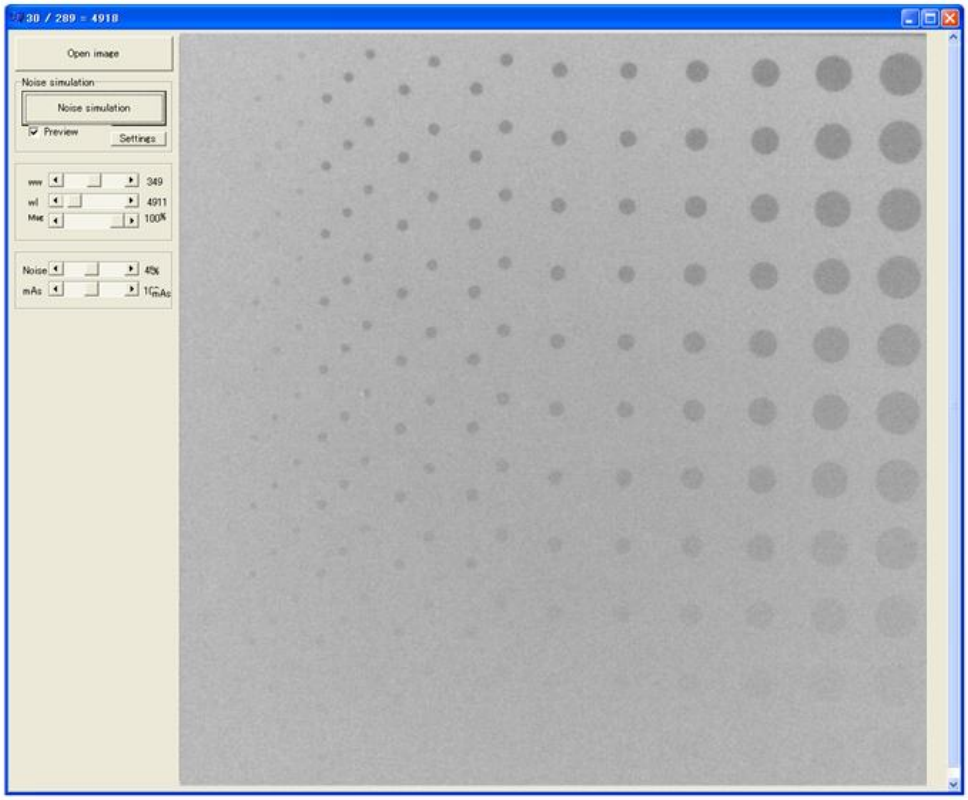


Figure 5 Graphic user interface of our system

## REFERENCES

1. International electrotechnical commission, IEC International standard 61267 Medical diagnostic X-ray equipment-Radiation conditions for use in the determination of characteristics. Geneva, Switzerland: IEC (1994)
2. International electrotechnical commission, IEC International standard 62220-1. Medical diagnostic X-ray equipment-Characteristics of digital imaging devices-Part 1: Determination of the detective quantum efficiency. Geneva, Switzerland: IEC (2003)
3. International commission on radiation unit and measurement (ICRU). Tissue substitutes in radiation dosimetry and measurement. ICRU report 44, Bethesda, MD, USA: ICRU (1989)
4. Brandrup J, Immergut EH, and Grulke EA. Polymer handbook (4th edn), New York, USA: Wiley-Interscience (2003)
5. Dainty JC, and Shaw R. Image Science. London, UK: Academic Press (1974)
6. Walter H. Review of radiologic physics (3rd edn), Philadelphia, USA: Lippincott Williams & Wilkins (2010)
7. Samei E, Hill JG, Frey GD, et al., "Evaluation of a flat panel digital radiographic system for low-dose portable imaging of neonates," Med Phys 30(4), 601-7 (2003)

## REFERENCE LINKING

[1] International electrotechnical commission (IEC), [International standard 61267 Medical diagnostic X-ray equipment-Radiation conditions for use in the determination of characteristics], IEC, Geneva Switzerland, (1994).

[2] International electrotechnical commission (IEC), [International standard 62220-1. Medical diagnostic X-ray equipment-Characteristics of digital imaging devices-Part 1: Determination of the detective quantum efficiency], IEC, Geneva Switzerland, (2003).
[3] International commission on radiation unit and measurement (ICRU), [Tissue substitutes in radiation dosimetry and measurement. ICRU report 44], ICRU, Bethesda MD USA, (1989).
[4] Brandrup J, Immergut EH, and Grulke EA., [Polymer handbook (4th edn)], Wiley-Interscience, New York USA, (2003).
[5] Dainty JC, and Shaw R., [Image Science], Academic Press, London UK, (1974).
[6] Walter H., [Review of radiologic physics (3rd edn)], Lippincott Williams & Wilkins, Philadelphia USA, (2010).
[7] Samei E, Hill JG, Frey GD, et al., "Evaluation of a flat panel digital radiographic system for low-dose portable imaging of neonates," Med Phys 30(4), 601-7 (2003).